Water Resources Research

Fine Sediment Deposition and Filtration Under Losing and Gaining Flow Conditions: A Particle Tracking Model Approach

Antonio Preziosi-Ribero[1] , Aaron I. Packman[2] , Jorge A. Escobar-Vargas[1,3],
Colin B. Phillips[2] , Leonardo David Donado[1] , and Shai Arnon[4]

[1]Facultad de Ingeniería, Universidad Nacional de Colombia, Bogotá,Colombia, [2]Department of Civil and Environmental Engineering, Northwestern University, Evanston, IL, USA, [3]Departamento de Ingeniería Civil, Pontificia Universidad Javeriana, Bogotá, Colombia, [4]Zuckerberg Institute for Water Research, the J. Blaustein Institutes for Deseart Research, Ben-Gurion University of the Negev, Beersheba, Israel

Abstract Fine particle deposition within riverbeds plays a major role in riverine ecology and biogeochemistry by altering hyporheic exchange flux. Moreover, it is ubiquitous within streams and rivers across all flow stages. However, the dynamics of fine particle deposition are still not completely understood in rivers, and continuum models like the advection dispersion equation require modifications to represent the processes accurately. To enhance understanding of fine particle dynamics, we developed a novel numerical particle tracking model that simulates fine particle deposition as a stochastic process under losing, neutral, and gaining streamflow conditions. These flow conditions generate three different velocity profiles by combining the free surface and groundwater flows. In addition, a novel aspect of our model is the storage of filtered particles to estimate concentration fields within the bed. Our simulated results are qualitatively compared with previous laboratory flume experimental results of kaolinite deposition under similar conditions. The model indicates that fine particle deposition patterns and residence time functions depend heavily on the exchange flux between stream and groundwater, as well as bed filtration properties as the deposition of particles occurs at greater depths in the losing stream condition than in the neutral and gaining cases. Therefore, the spatial pattern of particle deposition is a direct result of pore water velocity profiles, while the concentration depends on filtration dynamics within the bed.

1. Introduction

Rivers integrate over a host of catchment processes representing collections of different geological, biological, chemical, and ecological phenomena (Boano et al., 2014). Many of these phenomena depend on the exchange of momentum, matter, and energy between the river and the underlying sediments (see Boano et al., 2014and references therein). Streamflow into and back out of the subsurface is commonly termed hyporheic exchange (HE) and can occur across a range of different scales with varying magnitudes (Buendia et al., 2014; Stonedahl et al., 2010). HE is affected by fine particle transport and deposition within the stream because of filtering processes present in the riverbed that can lead to clogging and siltation (Crenshaw et al., 2002; Fox et al., 2018; Mendoza-Lera et al., 2017). This interaction between sediment transport and deposition can alter nutrient fluxes in rivers and plays an important role in determining the integrity of the aquatic ecosystem as a whole (Partington et al., 2017). Indeed, contaminant transport and carbon and nutrient dynamics are closely related to HE and sediment deposition (Gottselig et al., 2014; Hope et al., 1994).

Fine particle deposition, ubiquitous within rivers systems, is driven by the interactions of surface flow and bed morphology (Harvey et al., 2012; Packman et al., 2000a, 2000b). Suspended particles in rivers are typically minerals or aggregations of organic matter with sizes smaller than 10 μm (Drummond et al., 2014, 2018; Harvey et al., 2012; Huettel et al., 1996; Jin et al., 2019). Fine particles, due to their small size and density, are easily suspended in water (Packman et al., 2000a). However, they may deposit through interactions with geomorphic features which induce hyporheic flow such as dunes, pools, riffles, and bars (Buendia et al., 2014). Moreover, they are well known to deposit in the stream bed and resuspend into the surface flow with some periodicity (Cushing et al., 1993; Drummond et al., 2015; Karwan & Saiers, 2012; Newbold et al., 2005)

depending on variations of surface flow conditions, which can be driven by natural floods or the release of water from dams (Drummond et al., 2017). Additionally, fine particle retention in the stream bed is known to affect hyporheic flow, the exchange of nutrients, and alter physical properties of the media like porosity and permeability (Crenshaw et al., 2002; Dong et al., 2012; Karwan & Saiers, 2009; Mendoza-Lera et al., 2017; Newbold et al., 2005; Packman & MacKay, 2003; Simpson & Meixner, 2012; Thomas et al., 2001).

Enhanced fine particle loading in streams and thus increased deposition have recently been fostered by land use changes (Gartner et al., 2012; Wohl, 2015). This increased deposition impacts biogeochemical processes such as nutrient and carbon cycling (Gottselig et al., 2014; Hope et al., 1994) through the reduction of HE as particles clog the riverbed (Brunke, 1999). Indeed, fine particle deposition and transport affect the growth of microbial communities and favor denitrification processes due to the lack of oxygen in clogged zones (Navel et al., 2011). Thus, the understanding of fine particle dynamics in riverbeds is a challenge for river restoration and management.

In part due to the complexity of natural rivers, laboratory experiments have represented one of the primary tools for understanding the coupling between HE and sediment deposition (Elliott & Brooks, 1997b; Marion et al., 2002; Salehin et al., 2004). An important insight gained from early experimental efforts suggests that fine particle deposition occurs not only by gravitational deposition (Vanoni, 1974) but also by other key physical parameters. Flume models are ideal systems for studying local scale processes and isolating specific mechanisms for understanding the coupling between HE and sediment deposition. Understanding the role of regional groundwater patterns that result in losing and gaining flow conditions on fine sediment deposition has, to date, only been evaluated in relatively small number of experiments (Chen et al., 2013; Dong et al., 2012; Simpson & Meixner, 2012).

At the reach scale, the exchange between surface flows and groundwater has been heavily recorded and modeled (Cardenas et al., 2004; Cardenas & Wilson, 2006; Fox et al., 2014; Harvey et al., 2012; Hester et al., 2013; Marzadri et al., 2016; Woessner, 2000). The results of these observations and simulations suggest that the riverbed acts as a filter that traps a variety of fine particles through different mechanisms (i.e., filtration and straining). Another relevant result is that particle deposition changes the physical properties of the riverbeds, like porosity and permeability. However, reach-scale models are not able to accurately quantify the effects of groundwater flow on sediment deposition patterns at small scales. Thus, it is necessary to explore further this aspect to validate how the interaction between free surface flow and groundwater flow hinders or fosters sediment deposition in streams.

Particle deposition has been assessed under the assumptions of the advective pumping model in numerical simulations, generating flow paths in the stream bed due to the change of pressure generated by the presence of ripples and dunes (Elliott & Brooks, 1997a, 1997b). Some of these models have focused on estimating hydrodynamic fields and solute transport using continuum mechanics expressions such as the advection dispersion equation (ADE) (Boano et al., 2007; Cardenas & Wilson, 2006, 2007a, 2007b; Cardenas et al., 2008; Trauth et al., 2013). Models that use numerical particles that represent fine sediments have also been used to assess deposition patterns through the use of measured velocity profiles at local scales (Packman et al., 2000a). The particle tracking (PT) approach can also be used at reach scales to model nutrient uptake in rivers (Li et al., 2017). Advantage of using PT models is that this technique is useful for a wide range of scales (Delay et al., 2005) and that physical and chemical processes can be included and analyzed separately. However, modeling the physical process of particle deposition under different groundwater flow conditions remains a major challenge for river systems, since current models do not include explicit terms that account for vertical groundwater flow. Therefore, estimating the effect of particle deposition and HE remains imprecise.

This paper aims to present a PT model that assesses fine sediment deposition under losing or gaining streamflow conditions. This is a novel approach, since it explores the macroscopic process of flow in porous media due to the advective pumping model and through the incorporation of a discrete probabilistic framework that simulates the filtration process within the bed. By implementing this model, new information is gained regarding on the accumulation patterns of particles under neutral, upflow, and downflow conditions. Moreover, these results show that our model can be used as a direct comparison of fine particle deposition in systems with regular sand beds under losing and gaining streamflow conditions.
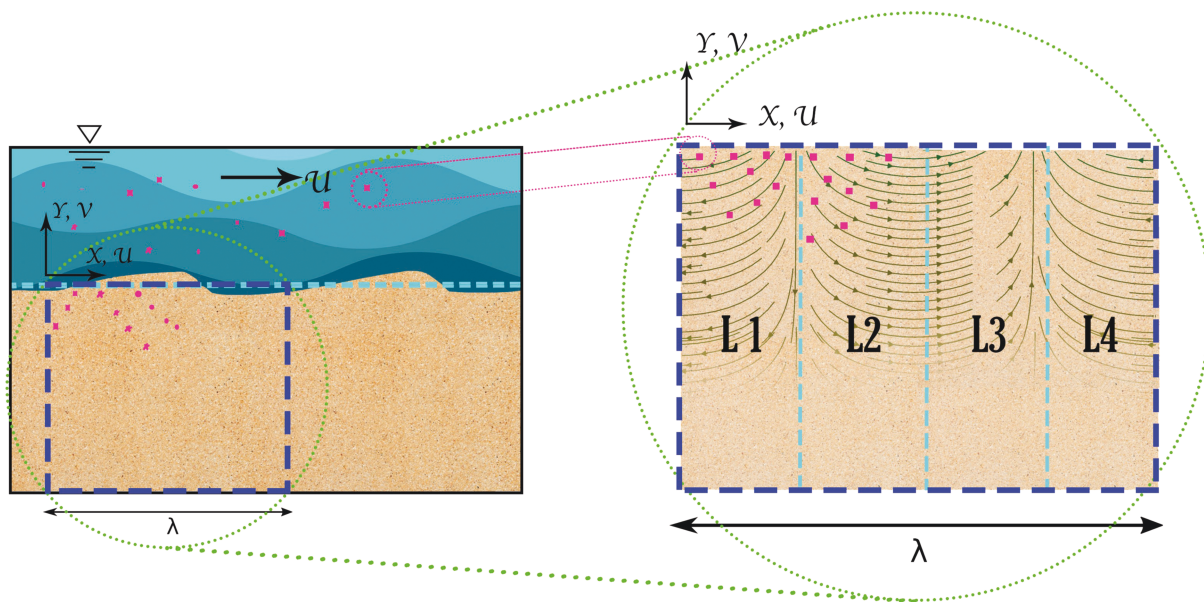
Figure 1. Conceptual model. Left: Sand bed with dune-shaped bedforms. The blue box outlines the model domain (λ is the characteristic dune's wavelength). The cyan dashed line demarcates the mean height of the bed. Right: Zoom of the model domain. Idealized streamlines from velocity profiles. Note that the lateral boundary conditions of the model are periodic. Particles (pink rectangles) are seeded at the top of the domain in the left half of the dune, propagate through the bed, and are filtered within bed sediments. The domain is divided into four locations (L1 to L4) to compare the deposition patterns with the experiments from Fox et al. (2018).

2. Methods

2.1. Conceptual Model

The PT model aims to represent instantaneous fine sediment deposition dynamics within an idealized sand bed with periodic bedforms and variable groundwater flow patterns (Figure 1). The conceptual model framework follows the work by Elliott and Brooks (1997a, 1997b), Packman et al. (2000a), and Packman and Bencala (2000), while the groundwater flows represent conditions that were used in the experimental setup within the work of Fox et al. (2014, 2018). Our numerical PT model builds on the framework of Li et al. (2017) developed to understand nutrient transport in rivers. However, for this case the particles are recorded at every time step to assess the deposition patterns within the domain. Here we impose a gaining or losing flux at the bottom of the model domain as a superposition of the velocity field generated from the advective pumping model (Elliott & Brooks, 1997a). The geomorphological and hydrologic flow conditions within the numerical model most closely represent a two-dimensional simplification of the experimental conditions within previous studies on fine particle deposition (Fox et al., 2014, 2018; Packman et al., 2000a) (Table 1). However, these features are fairly typical of natural sand bed systems (Chen et al., 2013; Dong et al., 2012; Harvey et al., 2012; Hünken & Mutz, 2007; Mutz, 2000; Mutz & Rohde, 2003; Simpson & Meixner, 2012; Vanoni, 1974; Wörman et al., 2007). To further generalize the model, nondimensional quantities are used for the comparisons.

The primary assumptions within the model are (i) macroscopic processes are considered separately from pore-scale processes; hence, the movement of the particles is considered independent from the bed filtration process; (ii) particles do not interact with each other; (iii) particles do not change the flow conditions in the media when they are filtered in the bed; (iv) fine particle deposition is irreversible; and (v) the shape of the dune is replaced by a sinusoidal pressure applied at the top of the domain. From experiments we know that these assumptions are not always valid, as particle collisions can lead to larger agglomerates and particle clogging can alter flow paths (Fox et al., 2018). However, since the particle injection is instantaneous and the flow conditions are permanent, alteration of the velocity field is not taken into account. In the case of a continuous particle injection, the alteration of flow paths would depend on particle deposition through a feedback cycle between the velocity field and filtration within the domain.

The horizontal model computational domain represents a single dune wavelength (λ) (Figure 1). In the vertical axis, the domain has a side d_b that stands for the depth of the sand bed or the distance between the

Table 1
Physical Parameters (Fox et al., 2014, 2018; Packman et al., 2000a) for the Comparison of the Implemented Particle Tracking Model

Physical parameters	Symbol	Value
Flume width (cm)	W	29.0
Sediment porosity (-)	θ	0.33
Hydraulic conductivity (cm/s)	K	0.12
Flow (L/min)	Q	261.0
Mean stream velocity (cm/s)	U	15.0
Sediment depth (cm)	d_b	20.0
Dune wavelegth (cm)	λ	15.0
Water depth (cm)	d	8.8
Total streambed area (cm^2)	A	15.1
Imposed vertical flux (in/out) (cm/day)	q_{in}	±12.5
Filtering coefficient (1/cm)	λ_f	0.6

free surface flow and an impervious layer at the bottom of the domain. For practical purposes the width of the sand bed was modeled according to experimental values reported (Fox et al., 2014, 2018). The sides of the box are open, and they represent periodic boundary conditions as particles that exit the domain on the right will reenter on the left boundary and vice versa (Figure 1).

The free surface model flow conditions are approximated by combining the advective pumping model (Elliott & Brooks, 1997a) with each groundwater flow condition (i.e., losing, neutral, or gaining). This model estimates the velocity field within the bed as a result of pressure variations at the top of the sand dunes that form the riverbed. The particles are seeded at the top of the domain in the left half ($\lambda/2$), which conceptually represents the upstream (stoss) side of the sand dune. The particle injection is instantaneous and performed before the first time step of the model. In each time step, the introduced particles travel according to the estimated velocity field followed by a filtration step represented as a random process. Sections 2.2 and 2.3 explain in detail the particle mobility and trapping/filtering features of the model.

2.2. Mathematical Model

The velocity fields used to model the water flow inside the dune are taken from existing literature (Elliott & Brooks, 1997a; Packman et al., 2000a) with an additional superimposed groundwater flow component (equations (1) and (2)). The groundwater vertical flow condition represents a positive upward velocity for the gaining condition and negative downward velocity for the losing condition.

$$u(x, y) = -(kKh_m)\cos(kx)[\tanh(kd_b)\sinh(ky) + \cosh(ky)] \tag{1}$$

$$v(x, y) = -(kKh_m)\sin(kx)[\tanh(kd_b)\cosh(ky) + \sinh(ky)] \pm q_{in/out} \tag{2}$$

where x and y represent the Cartesian coordinate reference axis ($x > 0$ for the downstream direction and $y = 0$ at the top of the domain), k is the normalized dune wavelength ($2\pi/\lambda$), and u and v are the horizontal and vertical velocity components, respectively. Furthermore, h_m represents the mean pressure over the dune, K stands for the permeability of the media, d_b for the thickness of the bed, and $q_{in/out}$ is the component of vertical velocity caused by the groundwater inflow/outflow.

We normalized all of the quantities and parameters according to theory developed for flow and transport in sand beds (Elliott & Brooks, 1997a; Packman et al., 2000a). As a result, equations (1) and (2) are transformed in equations (3) and (4). The inflow/outflow velocity $q_{in/out}$ is normalized by the maximum pumping velocity u_m. The addition of the vertical velocity alters the flow directions within the domain and introduces areas of flow recirculation and stagnation absent in the neutral flow condition velocity profiles (Figures 2a–2c). The neutral velocity profile (Figure 2b) shows streamlines starting and ending in two vertical streamlines that enter and leave the domain at $-\pi/2$ and $\pi/2$. For the losing flow condition (Figure 2a) the vertical streamline that enters the domain at $\pi/2$ remains unaffected in its shape. However, the vertical streamline at $-\pi/2$ is shortened due to the presence of the downward imposed flux. This feature generates a recirculation zone that enhances vertical downward flux and hinders the upward flux that leaves the domain. Instead, for the
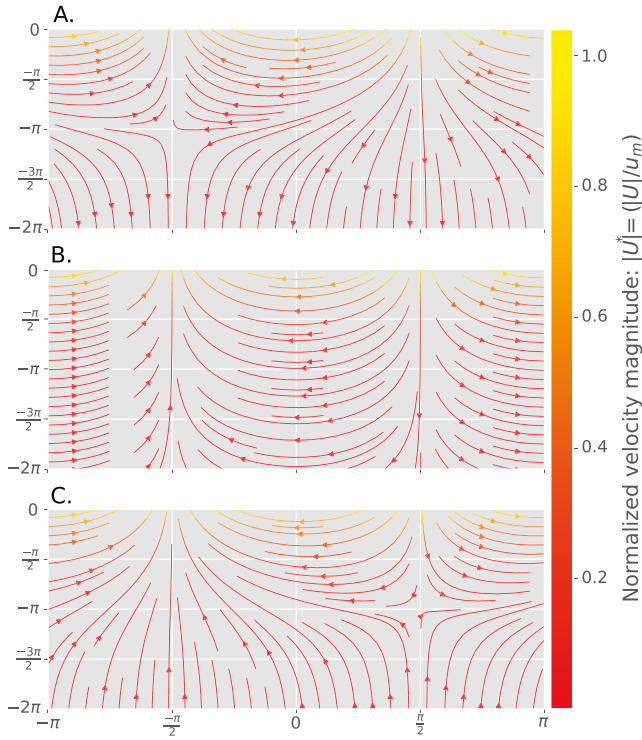
Figure 2. Streamlines for losing (a), neutral (b), and gaining (c) flow conditions. Domains are plotted in the interval $[-\pi/2, \pi/2]$ as each domain is periodic. The color bar represents the magnitude of the velocity vector. Vertical and horizontal axes not to scale.

gaining flow condition (Figure 2c), the vertical streamline located at $\pi/2$ going downward is shortened and the streamline at $-\pi/2$ going upward is enhanced by the groundwater flow condition.

$$u^*(x^*, y^*) = -\cos(x^*)[\tanh(d_b^*)\sinh(y^*) + \cosh(y^*)] \tag{3}$$

$$v^*(x^*, y^*) = -\sin(x^*)[\tanh(d_b^*)\cosh(y^*) + \sinh(y^*)] \pm q_{\text{in/out}}^* \tag{4}$$

The resulting velocity fields generated with the superposition of the advective pumping model and the vertical groundwater flow are physically reasonable, as the lowest velocities are present at the bottom of the domain where the influence of the surface flow has been reduced and the vertical groundwater flow prevails. At the top of the domain, the opposite happens, that is, the flow field is highly affected by surface flow conditions and the effects of the imposed groundwater flow are less evident. We can assess the particle path behavior relative to the velocity profiles through the Stokes number, which is defined as the relation between the stopping distance and the characteristic length of the phenomenon (equation (5)) (Clark, 2009; Ren & Packman, 2002).

$$Stk = \frac{\rho_p d_p^2 u_0}{18\mu_f l_0} \tag{5}$$

where ρ_p is the particle density taken here as that of kaolinite ($2{,}650 \frac{\text{kg}}{\text{m}^3}$), $d_p = 384 \times 10^{-6}$ m is the mean diameter (Fox et al., 2014), $u_0 = 0.01 \frac{\text{m}}{\text{s}}$ is the mean velocity in the subsurface, $\mu_f = 1.519 \times 10^{-3}$ Pa s is the dynamic viscosity of water (Cengel & Cimbala, 2006), and $l_0 = 0.01$ m is a characteristic length of the phenomenon which is taken as the dune's height (Fox et al., 2018). With a Stokes number $Stk = 0.014$ less than 1.0 we expect clay particles to follow streamlines and thus our model particles track the velocity profile streamlines described in equations (3) and (4) (Schulz, 2007). Settling velocity is neglected for this experiment under the assumption that particle diameters are small and enter the bed at low velocities to ensure a low Stokes number such that they will follow the streamlines generated by the velocity fields (Ren & Packman, 2002). While not implemented here, the model framework is able to take into account this feature. The mathematical model starts with the transport of particles along given streamlines, that is, the ADE (equation (6)).

$$\frac{\partial C}{\partial t} + u(x,y)\frac{\partial C}{\partial x} + v(x,y)\frac{\partial C}{\partial y} = D\left(\frac{\partial^2 C}{\partial x^2} + \frac{\partial^2 C}{\partial y^2}\right) - S \tag{6}$$

Here, C stands for the concentration of the particles, u and v for the horizontal and vertical velocities, respectively, D for the mechanical dispersion coefficient, and S for rate of particles removal due to filtration (Packman, 1997). The dispersion process for colloids with diamters <2 μm can be neglected in particle transport in porous media (Boano et al., 2014; Domenico & Schwartz, 1998; Packman et al., 2000a; Ren & Packman, 2002). Therefore, the ADE can be transformed into an equation that represents a filtration process over a given velocity field (equation (7)). Here, the local and advective acceleration equals the rate of removal of particles over time.

$$\frac{DC}{Dt} = \frac{\partial C}{\partial t} + u(x,y)\frac{\partial C}{\partial x} + v(x,y)\frac{\partial C}{\partial y} = -S \tag{7}$$

The rate of particle removal S can be expressed with the aid of the filtration coefficient λ_f, the seepage velocity $U = \partial s/\partial t$ (where s is the path traveled by the particle), and the concentration C of the analyzed particles as follows:

$$S = \lambda_f \frac{\partial s}{\partial t} C \tag{8}$$

Combining (8) with equation (7), the expression for particle filtering becomes

$$\frac{\partial C}{\partial s} = -\lambda_f C \qquad (9)$$

This model formulation is consistent with previous models of colloidal transport in porous media (Domenico & Schwartz, 1998). The key outcome of the mathematical model is that a filtration process along steady streamlines can be expressed as a first-order removal rate. In other words, the stochastic framework for filtration is applied using a removal constant (λ_f) to estimate the probability (p) that each particle has been filtered while traveling along a flow path (see section 2.3).

2.3. Numerical Model

The proposed numerical model is similar to the one used by Packman et al. (2000a). Its logical process is divided in three parts that use the discrete versions of equations (7) and (9). The initial step calculates the displacement of particles using the Taylor series expansion $x(t + \Delta t) = x(t) + u \cdot \Delta t$ (Li et al., 2017). In each time step the model takes into account the particles' previous positions and determines their velocities based on the velocity field.

After estimating each particle's position, the filtration process over the time step is estimated by calculating the probability p that the particle stops inside the domain (Prickett et al., 1981). This is provided by generating a random number (n) for each particle and comparing the random number with the λ_f and the distance traveled by the particle over the time step (Δs).

$$p = 1 - e^{-\lambda_f \Delta s} \approx \lambda_f \Delta s \qquad (10)$$

This assumption is justified as the size of the time step Δt is small enough to ensure the validity of Taylor's expansion (Li et al., 2017). At the end of every time step particles within the domain are counted and divided into two categories: (i) filtered particles that will remain immobile for the remainder of the simulation and (ii) mobile particles which have not been filtered. Particles that leave the domain out of the top boundary are accounted for as escaped particles that do not return to the domain during the simulation.

The particle tracking simulations were performed under the conditions proposed in Table 1. The cases were modeled with 2×10^5 particles for each vertical flow condition (losing, neutral, and gaining). The total simulation time ensured that all of the seeded particles were either filtered or escaped the domain by the end of the simulation. As regards to the initial condition, the particles are seeded uniformly across the left half of the top of the domain ($0 < x^* < \pi$) within the imposed downwelling flow due to HE. Particles are not seeded on the right part of the domain ($\pi < x^* < 2\pi$) as the upwelling flow from HE would result in these particles immediately escaping the domain (2).

To compare the PT model with the experimental results (Fox et al., 2014, 2018), the model domain is superimposed with a mesh of 100×167 squares of size $\pi/50$. Then, particles are binned and counted in each square. The resolution of the mesh was selected according to the experimental framework to be able to compare the number of particles in our model with clay concentration of the experiments. It is worth mentioning that the mesh used for counting particles has no relationship with the computational PT simulation as it is only used for particle counting purposes (Xue et al., 2017).

The numerical model is implemented in Matlab via a primary script that performs the individual PT and stores the particles' locations in a range of time selected by the user. For the case of each model run, particles' coordinates were stored every 10 time steps. After the PT model run, the output coordinates are read by a Python script that counts particles inside the superimposed mesh to generate particle maps and process information over space and time. The primary results that are analyzed are from particle counting rather than the raw PT model results. Model codes are freely available (see acknowledgments).

To estimate the residence time function (RTF), that is, the fraction of particles injected in the bed at a time t_0 and still present within the domain in a given time t (Packman et al., 2000a), particles are separated into three categories during a run: (traveling particles, ii) filtered particles, and (iii) particles that escaped the domain. For any given time step, the RTF is the result of sum of particles that are traveling through the domain with the particles that have been previously filtered. The result is then normalized by the total number of particles seeded at the beginning of the model.
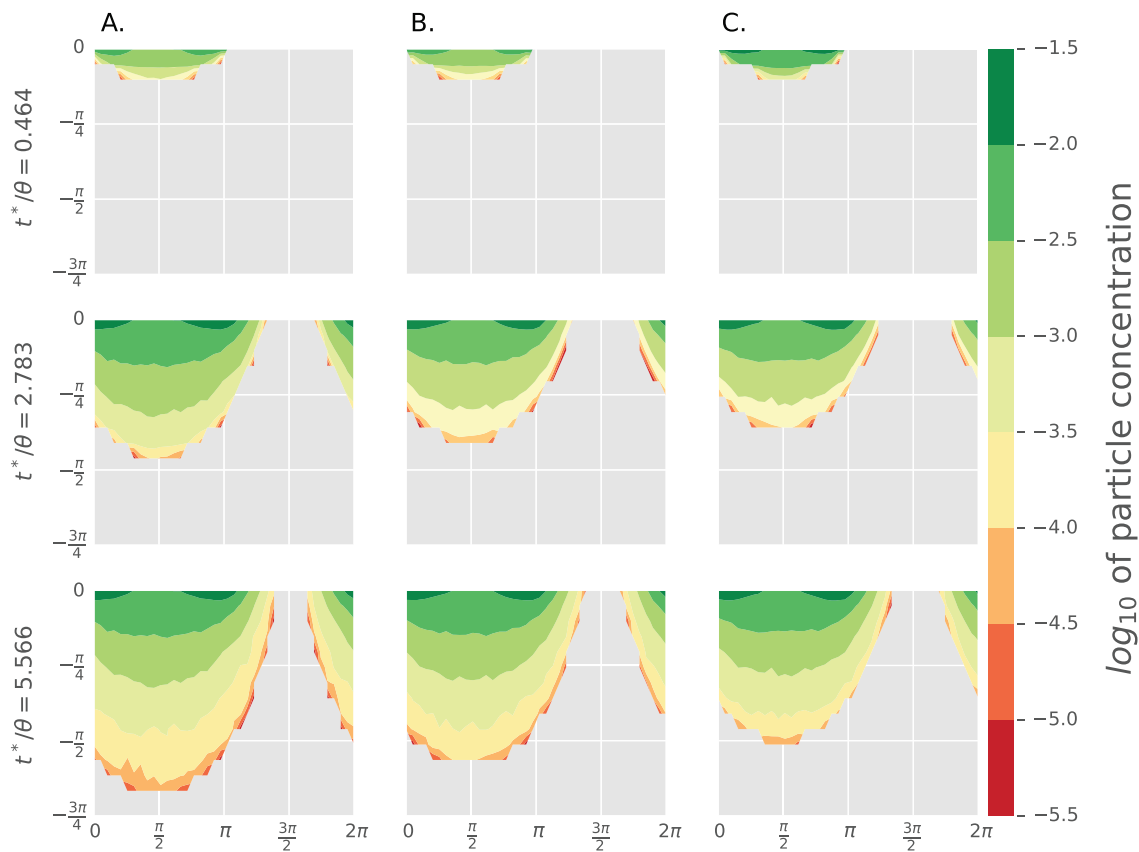
Figure 3. Logarithm of the total number of particles deposited for different times (rows) and under different inflow/outflow conditions (columns). (a) Losing condition, (b) neutral condition, and (c) gaining condition (Note that axes are not to scale).

3. Results

The pore water flow patterns under losing, neutral, and gaining streamflow conditions that result from equations (3) and (4) (Figure 2) show substantial differences (Figure 2). Preferential flow paths going upward or downward occur when the imposed condition is a gaining or losing flow, respectively. The addition of vertical flow (losing/gaining) to the neutral flow condition creates an area of no net flow across the sediment-water interface that corresponds to the top part of the domain. For the losing case, this area is located at the lee side of the dune ($-\pi/2$) and for the gaining condition on the stoss side ($\pi/2$). In these areas there is no flow at all because of the superposition of the advective pumping model with the groundwater vertical flow condition. In addition, the areas of no flow create a corresponding recirculation zone in the losing and gaining cases (locations can be seen in Figure 2a in the coordinates ($-\pi/2, -\pi$) and C in the coordinate ($\pi/2, \pi$)). These recirculation zones are expected to trap any particles that are able to reach them.

Due to the altered losing and gaining flow conditions, the maximum velocities in each profile are located in different places. In particular, in the losing condition the maximum velocity is into the bed (negative) on the stoss side (upstream) of the domain, while in the gaining case it is located in dune's lee (downstream). However, in the neutral condition the maximum velocities are located in two parts of the domain but with opposite signs, with downwelling on the lee ($-\pi/2$) and the upwelling on the stoss ($\pi/2$) side. Even though particles follow the streamlines of the pore water flow patterns, their deposition is not uniform due to the inflow position on the upstream side of the dune's stoss side and filtering along the streamlines.

During early simulation times, the fine particle deposition patterns are generally similar in shape for the three modeled cases, though the concentrations differ (Figure 3 first row). For example, in the gaining condition the particles in the uppermost part of the domain are more evenly distributed than in the neutral and losing cases. At later times, the flow pattern due to advective pumping remains prominent as the area of
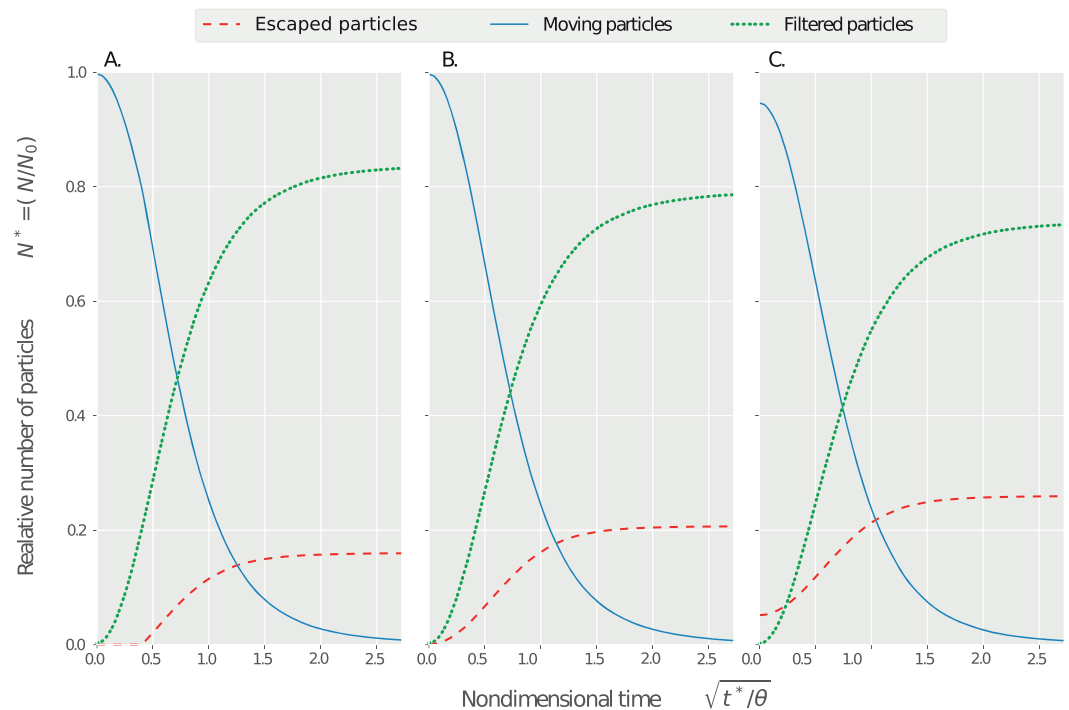
Figure 4. Behavior of escaped (dashed red line), moving (solid blue line), and filtered (dotted green line) particles over time. (a) Losing condition. (b) Neutral condition. (c) Gaining condition.

return flow is free of particles. However, the distribution of return flow is modified by the imposed vertical flow conditions; in the losing case it is significantly narrower than in the neutral and gaining ones (Figure 3).

With the PT model we can assess the particles behavior over time (Figure 4), because we record the relative number of mobile, filtered, and escaped particles within the domain (Figure 4). Even though each flow condition has the same filtration coefficient, the amount of particles that remain in the domain and escape from it varies appreciably between the imposed vertical flow conditions. Each one of the vertical flow conditions has characteristic curves of filtered, mobile, and escaped particles (Figure 4). For the losing case the fraction of filtered particles at the end of the simulation is 0.82, while it is 0.78 and 0.76 for the neutral and gaining cases, respectively. Conversely, 0.17, 0.20, and 0.24 of particles escaped the domain under the losing, neutral, and gaining cases, respectively. The behavior of the escaped, mobile, and filtered particles over time presents the same pattern between flow conditions, although there is a marked delayed onset of escaping particles in the losing flow condition. For gaining flow, however, some particles are initially lost upon seeding because they are carried out of the bed by upwelling water. In particular, the filtered particles present an exponential behavior in time, while the traveling and escaped particles have a monotonic increase until reaching a peak.

The PT model recovers the expected ensemble continuum behavior of fine particle deposition. The filtration process is expected to remove particles in an exponential way as a function of distance traveled by each particle, and this phenomenon is present in the model results. However, the presence of particles inside the domain is heavily conditioned by the vertical groundwater flow imposed. By tracking the number of remaining particles within the PT model, we can estimate a RTF. The three RTF were calculated as the fraction of particles that enter the bed near $t = 0$ and remain inside the domain after a given time τ (Elliott & Brooks, 1997a; Packman et al., 2000a). For small times, τ close to zero, the value of the RTF is 1.0; as τ increases some of the particles leave the domain and the RTF begins to decrease. Since the RTF is normalized by the total number of particles (Figure 5), the resulting curve is the complement of the cumulative distribution function ($1 - CDF$) of particles inside the domain.

The number of particles remaining within the domain depends on the vertical flow conditions. Neutral and gaining flow conditions have RTFs with very similar shapes, although under gaining flow fewer particles
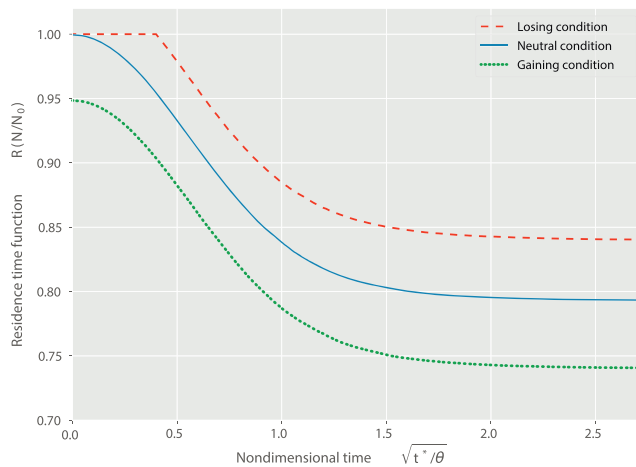
Figure 5. Residence time function for the different imposed flow conditions. The lines represent the complement of the cumulative distribution function ($1 - CDF$) of particles inside the domain at a time t^*/θ after the injection.

enter the bed from the start. Unlike the neutral and gaining flow conditions, under losing flow the RTF remains constant for a short period where all particles enter the bed and none have escaped yet. At longer timescales each RTF approaches a constant value. Although gaining and losing conditions have the same imposed flow speed but a different direction, the results of the RTF for the losing and gaining conditions are vertically shifted versions of the RTF curve of the neutral condition. To explore this, the residence time distributions for each time (Figure 6) were obtained by taking the gradient of each RTF and then applying a convolution between the derivative and a top hat function with unit area and a span of 400 points.

For all modeled cases, the probability of a particle leaving the domain is low at early times followed by an increase until the peak and then a monotonic decrease until all particles are removed or filtered. The time it takes the RTF to decrease at early times corresponds to the minimal path that a particle travels through the domain before exiting at the surface. For the losing case, this path is longer than for the neutral and gaining cases. Therefore, particles tend to remain inside the domain for more time, traveling longer distances inside, and are more prone to remain inside the domain (Figure 6 red line). This means that the probability of leaving the domain is lower for this case than for the neutral or gaining cases until reaching its peak value, again lower than for the two aforementioned cases. The primary difference between the three conditions occurs before the peak in the residence time distribution probability; after this point the three distributions are nearly identical (Figure 6).

We compare the PT model output with the experimental results from Fox et al. (2014, 2018). Experimental subsurface particle accumulation was sampled by coring each dune in triplicate at four equally spaced locations (1). Kaolinite mass was measured from the extracted cores at 0.5 cm intervals for each location. To facilitate the comparison between the experimental results and the PT model, we divide the nondimensional domain into sections of $\pi/2$ width. We then calculate the mean and standard deviation of the fraction of particles at each location (L1, L2, L3, and L4 from Figure 1 and compare the mass fraction of clay with the fraction of particles in every location (Figure 7). Our results show strong similarities with the experimental results. Particles deposit more in locations one and two (the stoss side of the dune) and show reduced deposition in locations three and four (lee side of the dune). The deposition in the latter locations occurs due to the particles following the hyporheic flow paths (Figure 2). There is good agreement between the PT model and the experimental results in the stoss of the sand dune (Figure 7 first two columns, locations 1 and 2 in
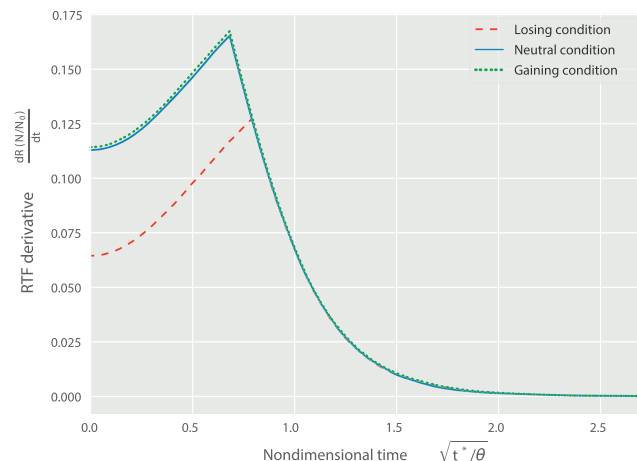
Figure 6. Derivative of RTF for the three vertical groundwater flow conditions modeled. These lines represent the Probability Density Function (PDF) of particles inside the domain at a given time t^*/θ after injection.
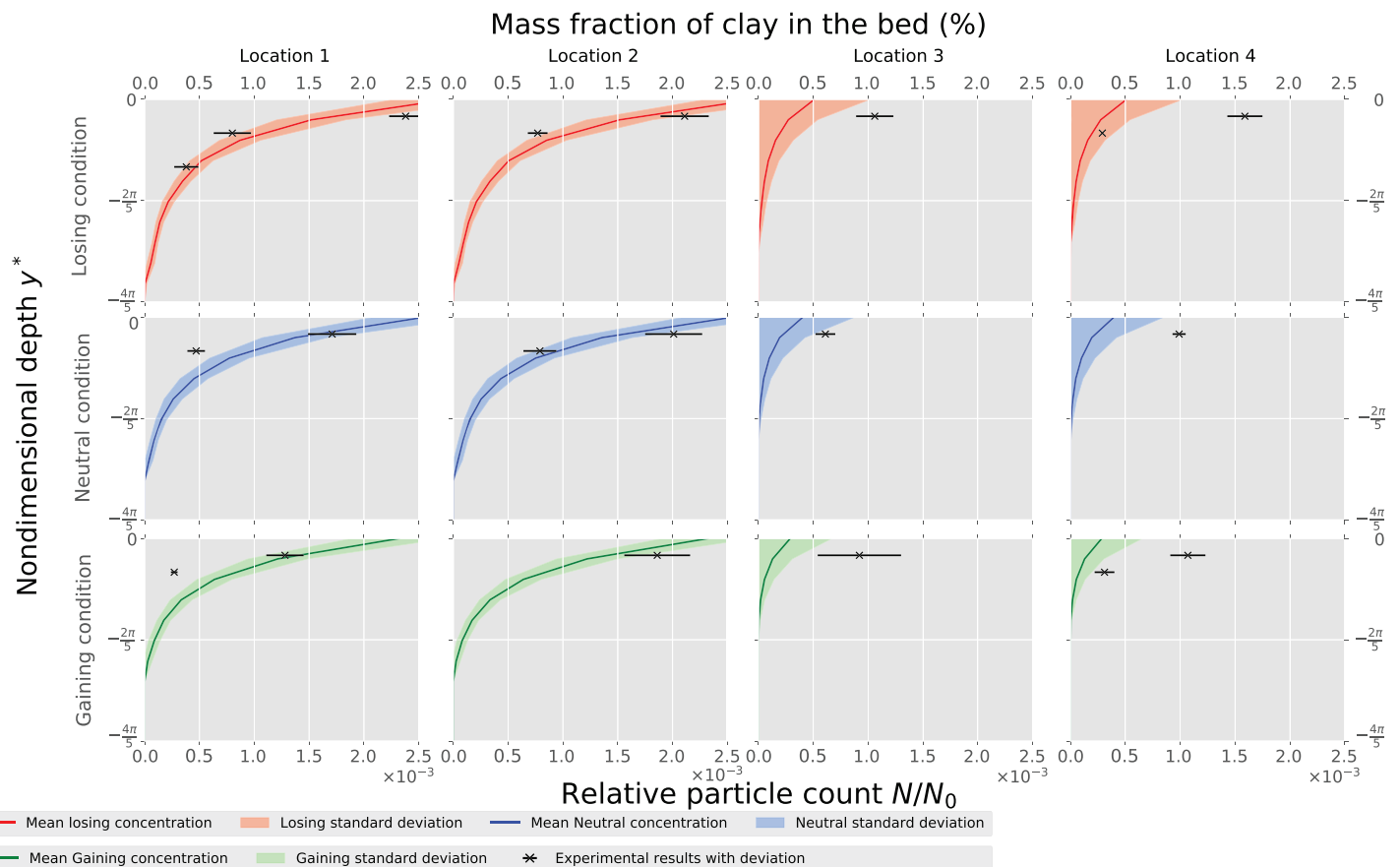
Figure 7. Comparison with experimental results from (Fox et al., 2018). The top horizontal axis represents the fraction of clay mass found in the experiments expressed in percent. The bottom horizontal axis represents the fraction of particles within the numerical domain. Solid colored lines and their corresponding shaded areas represent the average fraction and standard deviation of particles at each depth for the different locations. Crosses are the mean mass fraction sampled in the experiments, and black lines represent the standard deviation of the measurements.

right part of Figure 1). For each of the three flow cases modeled, the PT model underestimates the concentration of particles as the experimental results show more clay deposited with depth for locations 3 and 4 (Figure 7).

4. Discussion

The PT model developed here combines a continuum advective pumping hyporheic flow model with a stochastic filtration framework to simulate fine particle deposition within a sand bed. This is a novel approach that allows quantification of the fraction of mass deposited within a typical dune under homogeneous flow conditions. The superposition principle could be applied to estimate deposition behavior under different flow and injection conditions. Therefore, our results suggest that the model may be able to capture the macroprocesses of fine sediment deposition under losing, gaining, and neutral conditions. Additionally, our PT model framework does not pose any problems regarding mass conservation, artificial diffusion, or unwanted oscillations provoked by numerical scheme instabilities (Delay et al., 2005). The particle deposition and flow patterns are consistent with experiments and follow the expected mean continuum behavior, that is, our model captures the physical processes in a representative scale by simulating the combination between the pore-scale filtration and the macroscale advective pumping flow. Additions to the current modeling framework can be used to explore in further detail fine particle deposition phenomenon and patterns.

The Stokes number for each individual particle is low enough that it is safe to assume that the particles follow the streamlines. This assumption is supported due to the size of a typical clay particle and the maximum velocity which it is subject to when entering the streambed. Since the low Stokes number assumption

is validated for the maximum velocity, it holds for all lower velocities (equation (5)). Consequently, the phenomenon of settling velocity inside the sand bed is not taken into account as it was in previous works (Jin et al., 2019; Packman et al., 2000a).

The gaining flow condition produces less deposition than the neutral and losing condition (Figure 3). At early times the deposition is similar for all of the three modeled cases because the shallow streamlines have higher velocity; hence, they are barely altered by the groundwater flow. However, when particles travel to deeper parts, the groundwater and vertical flows become more important. The groundwater vertical flow imposed is estimated to be 8 % of the maximum pumping velocity u_m at the top of the domain. However, filtration is a function of each particle's displacement s; hence, deposition occurs primarily at the top of the domain in all of the modeled cases, because of the combination of velocity profiles generated by the dune shapes and the imposed vertical groundwater flow.

Important differences arise when comparing deposition patterns from the three conditions modeled as the depositional pattern depends on the overall combined subsurface velocity profiles. The deposition patterns (Figure 3) show that a change in the vertical flow conditions affects the maximum penetration depth of the particles and the horizontal extent of the particles. Not only more of particles deposit under the losing flow condition but the deposited particles will also cover a larger subsurface volume than the neutral and gaining cases (Figure 3).

The model-predicted decay of mean clay concentration with depth is similar to the experimental results presented by Fox et al. (2018), especially for the stoss side of the dune. Agreement between the PT model and the experimental results is poorer for the lee side of the bedform, and in general, the PT model standard deviation is less than that of the experimental results. The increased variability within the experimental results may be explained by differences in shape of the dunes in the experiment and the proposed idealized dune within the numerical model. Our model simulates an idealized dune with a fixed shape and constant physical properties inside the domain, while the shape of the dunes and the bed porosity are not homogeneous in the experiments.

The PT model is built on steady, continuum Darcy flow assumptions; hence, the effects of turbulent flows on the subsurface velocity patterns are not taken into account. In natural and laboratory cases, some of the total fine particle deposition occurs due to turbulence because of its ability to transport mass and momentum from the free flow stream to the porous media (Roche et al., 2018). Nevertheless, in sand beds the constrained pore spaces damp turbulence, making mean velocity fields and filtration dynamics the main drivers for deposition. This is also a relevant result in the experiments by Fox et al. (2018). However, our model is able to capture the main fine particle deposition phenomenon for this particular type of bed. For the case of cobble-bed flows with bigger spaces between grains, this model would not be suitable since the effects of turbulence from the free flow penetrate the bed, hence presenting unsteady flow effects (Manes et al., 2011; Packman et al., 2004).

In addition, changes in porosity (hence permeability) of the media due to the particles' deposition have been recorded in lab observations and numerical simulations (Chen et al., 2008), affecting the shape of the velocity fields under the different flow conditions. The change of bed porosity hinders HE in rivers and has visible effects on experimental HE patterns (Fox et al., 2018; Tonina et al., 2016). Our model provides a potential basis for simulating clogging processes in sand beds since it tracks the particles' position within the bed following a generated velocity field. However, effects on media heterogeneity are not taken into account within the current implementation. Nevertheless, heterogeneity in the porous medium can be considered using this particle tracking model approach, but that would require assumptions or observations regarding the structure of the bed and how the filtration coefficient varies within different types of sedimentary deposits. Our model focuses primarily on the main particle transport processes. Therefore, complexity associated with riverbed heterogeneity is beyond the scope of the current paper. Changes in permeability can be associated with the number of filtered particles within the domain. Afterward, a new transient flow field can be estimated to filter the remaining particles that move within the bed. However, there is a second-order effect of particle accumulation in the bed and it is the change in filtration coefficient due to the bed clogging. However, our results suggest that the proposed PT model is suitable to represent deposition patterns under different flow conditions.

Finally, natural streams are characterized by their heterogeneity in space and time; hence, our homogeneous sand bed PT model is not able to capture the fine particle deposition when compared to a more complex media made of different stratified materials like the ones found in natural streams. However, our results suggest that PT models remain a good approximation of observed fine particle deposition phenomenon and that this type of model is a good approximation for understanding how combined physical phenomena act as a whole in natural systems. Additionally, the validated behavior of particle filtration and transport within the bed allows for more complex phenomena to be added to the model, such as simulating the effects of chemical gradients or the presence of bio-active layers on nonconservative or reactive particles.

5. Conclusions

The implemented PT model showed substantial differences in the deposition profiles of fine particles in a sediment bed (figure 3). For the gaining flow condition the maximum penetration depth of the particles is less than in the neutral and losing cases, where the velocity fields push the particles further down within the domain. Our results suggest that the model captures the main physical processes of fine particle deposition within a streambed when combining the advective pumping model of a dune-shaped bed and the vertical groundwater flow conditions. Besides the maximum penetration of the particles within the domain, their spatial distribution is also different among cases, showing the combination of vertical flow conditions and filtration inside a sand bed. However, the particles' dynamics regarding the RTF of each case modeled show similarities, suggesting that the flow field shape and magnitude impact also the velocity of the particles while traveling across the domain. This effect is also seen in the presence of shallow zones with no particles inside the lee side of the modeled dunes. These zones are important for riverine biogeochemistry since they are the not occupied by fine particles that can obstruct the HE in natural systems composed of sand beds. Furthermore, these zones are present in experimental works done previously (Fox et al., 2014, 2018), showing that the proposed model is able to represent complex dynamics of particle deposition with results that are similar to the ones found both in flumes and natural systems.

References

Boano, F., Harvey, J. W., Marion, A., Packman, A. I., Revelli, R., Ridolfi, L., & Wörman, A. (2014). Hyporheic flow and transport processes: Mechanisms, models, and biogeochemical implications. *Reviews of Geophysics*, *52*, 603–679. https://doi.org/10.1002/2012RG000417

Boano, F., Packman, A. I., Cortis, A., Revelli, R., & Ridolfi, L. (2007). A continuous time random walk approach to the stream transport of solutes. *Water Resources Research*, *43*, W10425. https://doi.org/10.1029/2007WR006062

Brunke, M. (1999). Colmation and depth filtration within streambeds: Retention of particles in hyporheic interstices. *International Review of Hydrobiology*, *84*(2), 99–117.

Buendia, C., Gibbins, C. N., Vericat, D., & Batalla, R. J. (2014). Effects of flow and fine sediment dynamics on the turnover of stream invertebrate assemblages. *Ecohydrology*, *7*(4), 1105–1123.

Cardenas, M. B., & Wilson, J. L. (2006). The influence of ambient groundwater discharge on exchange zones induced by current bedform interactions. *Journal of Hydrology*, *331*(1-2), 103–109.

Cardenas, M. B., & Wilson, J. L. (2007a). Hydrodynamics of coupled flow above and below a sediment water interface with triangular bedforms. *Advances in Water Resources*, *30*(3), 301–313.

Cardenas, M. B., & Wilson, J. L. (2007b). Thermal regime of dune-covered sediments under gaining and losing water bodies. *Journal of Geophysical Research*, *112*, G04013. https://doi.org/10.1029/2007JG000485

Cardenas, M. B., Wilson, J. L., & Haggerty, R. (2008). Residence time of bedform-driven hyporheic exchange. *Advances in Water Resources*, *31*(10), 1382–386.

Cardenas, M. B., Wilson, J. L., & Zlotnik, V. A. (2004). Impact of heterogeneity, bed forms, and stream curvature on subchannel hyporheic exchange. *Water Resources Research*, *40*, W08307. https://doi.org/10.1029/2004WR003008

Cengel, Y. A, & Cimbala, J. M (2006). *Mecánica de fluidos : Fundamentos y aplicaciones*. México, D.F.: McGraw-Hill Interamericana, 2006.

Chen, X., Dong, W., Ou, G., Wang, Z., & Liu, C. (2013). Gaining and losing stream reaches have opposite hydraulic conductivity distribution patterns. *Hydrology and Earth System Sciences*, *17*(7), 2569–2579.

Chen, C., Packman, A. I., & Gaillard, J. F. (2008). Pore-scale analysis of permeability reduction resulting from colloid deposition. *Geophysical Research Letters*, *35*, L07404. https://doi.org/10.1029/2007GL033077

Clark, M. M. (2009). *Transport modeling for environmental engineers and scientists.*, Environmental science and technology. New Jersey: Wiley.

Crenshaw, C. L., Valett, H. M., & Webster, J. R. (2002). Effects of augmentation of coarse particulate organic matter on metabolism and nutrient retention in hyporheic sediments. *Freshwater Biology*, *47*(10), 1820–1831.

Cushing, C. E., Minshall, G. W., & Newbold, J. D. (1993). Transport dynamics of fine particulate organic matter in two Idaho streams. *Limnology and Oceanography*, *38*(6), 1101–1115.

Delay, F., Ackerer, P., & Danquigny, C. (2005). Simulating solute transport in porous or fractured formations using random walk particle tracking. *Vadose Zone Journal*, *4*(2), 360.

Domenico, P. A., & Schwartz, F. W. (1998). *Physical and chemical hydrogeology* (Second edition). New York: Wiley.

Dong, W., Chen, X., Wang, Z., Ou, G., & Liu, C. (2012). Comparison of vertical hydraulic conductivity in a streambed-point bar system of a gaining stream. *Journal of Hydrology*, *450-451*, 9–16.

Drummond, J. D., Davies-Colley, R. J., Stott, R., Sukias, J. P., Nagels, J. W., & Sharp, A. (2015). Microbial transport, retention, and inactivation in streams: A combined experimental and stochastic modeling approach. *Environmental Science and Technology*, *49*(13), 7825–7833.

Drummond, J. D., Davies-Colley, R. J., Stott, R., Sukias, J. P., Nagels, J. W., Sharp, A., & Packman, A. I. (2014). Retention and remobilization dynamics of fine particles and microorganisms in pastoral streams. *Water Research*, *66*, 459–472.

Drummond, J. D., Larsen, L. G., González-Pinzón, R., Packman, A. I., & Harvey, J. W. (2017). Fine particle retention within stream storage areas at base flow and in response to a storm event. *Water Resources Research*, *53*, 5690–5705. https://doi.org/10.1002/2016WR020202

Drummond, J. D., Larsen, L. G., González-Pinzón, R., Packman, A. I., & Harvey, J. W. (2018). Less fine particle retention in a restored versus unrestored urban stream: Balance between hyporheic exchange, resuspension, and immobilization. *Journal of Geophysical Research: Biogeosciences*, *123*, 1425–1439. https://doi.org/10.1029/2017JG004212

Elliott, A. H., & Brooks, N. H. (1997a). Transfer of nonsorbing solutes to a streambed with bed forms: Theory. *Water Resources Research*, *33*(1), 123–136.

Elliott, A. H., & Brooks, N. H. (1997b). Transfer of nonsorbing solutes to a streambed with bed forms: Laboratory experiments. *Water Resources Research*, *33*(1), 137–151.

Fox, A., Boano, F., & Arnon, S. (2014). Impact of losing and gaining streamflow conditions on hyporheic exchange fluxes induced by dune-shaped bed forms. *Water Resources Research*, *50*, 1895–1907. https://doi.org/10.1002/2013WR014668

Fox, A., Packman, A. I., Boano, F., Phillips, C. B., & Arnon, S. (2018). Interactions between suspended kaolinite deposition and hyporheic exchange flux under losing and gaining flow conditions. *Geophysical Research Letters*, *45*, 4077–4085. https://doi.org/10.1029/2018GL077951

Gartner, J. D., Renshaw, C. E., Dade, W. B., & Magilligan, F. J. (2012). Time and depth scales of fine sediment delivery into gravel stream beds: Constraints from fallout radionuclides on fine sediment residence time and delivery. *Geomorphology*, *151-152*, 39–49.

Gottselig, N., Bol, R., Nischwitz, V., Vereecken, H., Amelung, W., & Klumpp, E. (2014). Distribution of phosphorus-containing fine colloids and nanoparticles in stream water of a forest catchment. *Vadose Zone Journal*, *13*(7), 0005.

Hünken, A., & Mutz, M. (2007). Field studies on factors affecting very fine and ultra fine particulate organic matter deposition in low-gradient sand-bed streams. *Hydrological Processes*, *21*(4), 525–533.

Harvey, J. W., Drummond, J. D., Martin, R. L., McPhillips, L. E., Packman, A. I., Jerolmack, D. J., et al. (2012). Hydrogeomorphology of the hyporheic zone: Stream solute and fine particle interactions with a dynamic streambed. *Journal of Geophysical Research*, *117*, G00N11. https://doi.org/10.1029/2012JG002043

Hester, E. T., Young, K. I., & Widdowson, M. A. (2013). Mixing of surface and groundwater induced by riverbed dunes: Implications for hyporheic zone definitions and pollutant reactions. *Water Resources Research*, *49*, 5221–5237. https://doi.org/10.1002/wrcr.20399

Hope, D., Billett, M. F., & Cresser, M. S. (1994). A review of the export of carbon in river water: Fluxes and processes. *Environmental Pollution*, *84*(3), 301–324.

Huettel, M., Ziebis, W., & Forster, S. (1996). Flow-induced uptake of particulate matter in permeable sediments. *Limnology and Oceanography*, *41*(2), 309–322.

Jin, G., Zhang, Z., Tang, H., Xiaoquan, Y., Li, L., & Barry, D. A. (2019). Colloid transport and distribution in the hyporheic zone. *Hydrological Processes*, *33*(6), 932–944.

Karwan, D. L., & Saiers, J. E. (2009). Influences of seasonal flow regime on the fate and transport of fine particles and a dissolved solute in a New England stream. *Water Resources Research*, *45*, W11423. https://doi.org/10.1029/2009WR008077

Karwan, D. L., & Saiers, J. E. (2012). Hyporheic exchange and streambed filtration of suspended particles. *Water Resources Research*, *48*, 1–13. https://doi.org/10.1029/2011WR011173

Li, A., Aubeneau, A. F., Bolster, D., Tank, J. L., & Packman, A. I. (2017). Covariation in patterns of turbulence-driven hyporheic flow and denitrification enhances reach-scale nitrogen removal. *Water Resources Research*, *53*, 6927–6944. https://doi.org/10.1002/2016WR019949

Manes, C., Poggi, D., & Ridolfi, L. (2011). Turbulent boundary layers over permeable walls: Scaling and near-wall structure. *Journal of Fluid Mechanics*, *687*, 141–170.

Marion, A., Bellinello, M., Guymer, I., & Packman, A. I. (2002). Effect of bed form geometry on the penetration of nonreactive solutes into a streambed. *Water Resources Research*, *38*(10), 1209.

Marzadri, A., Tonina, D., Bellin, A., & Valli, A. (2016). Mixing interfaces, fluxes, residence times and redox conditions of the hyporheic zones induced by dune-like bedforms and ambient groundwater flow. *Advances in Water Resources*, *88*, 139–151.

Mendoza-Lera, C., Frossard, A., Knie, M., Federlein, L. L., Gessner, M. O., & Mutz, M. (2017). Importance of advective mass transfer and sediment surface area for streambed microbial communities. *Freshwater Biology*, *62*(1), 133–145.

Mutz, M. (2000). Influences of woody debris on flow patterns and channel morphology in a low energy, sand-bed stream reach. *International Review of Hydrobiology*, *85*(1), 107–121.

Mutz, M., & Rohde, A. (2003). Processes of surface-subsurface water exchange in a low energy sand-bed stream. *International Review of Hydrobiology*, *88*(34), 290–303.

Navel, S., Mermillod-Blondin, F., Montuelle, B., Chauvet, E., Simon, L., & Marmonier, P. (2011). Water-sediment exchanges control microbial processes associated with leaf litter degradation in the hyporheic zone: A microcosm study. *Microbial Ecology*, *61*(4), 968–979.

Newbold, J. D., Thomas, S. A., Minshall, G. W., Cushing, C. E., & Georgian, T. (2005). Deposition, benthic residence, and resuspension of fine organic particles in a mountain stream. *Limnology and Oceanography*, *50*(5), 1571–1580.

Packman, A. I. (1997). *Exchange of colloidal kaolinite between stream and sand bed in a laboratory flume* (Ph.D. Thesis), California Institute of Technology.

Packman, A. I., & Bencala, K. E. (2000). Modeling surface subsurface hydrological interactions, *Streams and ground waters* (pp. 45–80). San Diego, CA: Elsevier.

Packman, A. I., Brooks, N. H., & Morgan, J. J. (2000a). A physicochemical model for colloid exchange between a stream and a sand streambed with bed forms. *Water Resources Research*, *36*(8), 2351–2361.

Packman, A. I., Brooks, N. H., & Morgan, J. J. (2000b). Kaolinite exchange between a stream and streambed: Laboratory experiments and validation of a colloid transport model. *Water Resources Research*, *36*(8), 2363–2372.

Packman, A. I., & MacKay, J. S. (2003). Interplay of stream-subsurface exchange, clay particle deposition, and streambed evolution. *Water Resources Research*, *39*(4), 1097.

Packman, A. I., Salehin, M., & Zaramella, M. (2004). Hyporheic exchange with gravel beds: Basic hydrodynamic interactions and bedform-induced advective flows. *Journal of Hydraulic Engineering*, *130*(7), 647–656.

Partington, D., Therrien, R., Simmons, C. T., & Brunner, P. (2017). Blueprint for a coupled model of sedimentology, hydrology, and hydrogeology in streambeds. *Reviews of Geophysics*, *55*, 287–309. https://doi.org/10.1002/2016RG000530

Prickett, T. A., Naymik, T. G., & Lonnquist, C. G. (1981). A "random-walk" solute transport model for selected groundwater quality evaluations. Champaign: Illinois Department of Energy and Natural Resources.

Ren, J., & Packman, A. I. (2002). Effects of background water composition on stream subsurface exchange of submicron colloids. *Journal of Environmental Engineering*, *128*(7), 624–634.

Roche, K. R., Blois, G., Best, J. L., Christensen, K., Aubeneau, A. F., & Packman, A. I. (2018). Turbulence links momentum and solute exchange in coarse-grained streambeds. *Water Resources Research*, *54*, 3225–3242. https://doi.org/10.1029/2017WR021992

Salehin, M., Packman, A. I., & Paradis, M. (2004). Hyporheic exchange with heterogeneous streambeds: Laboratory experiments and modeling. *Water Resources Research*, *40*, W11504. https://doi.org/10.1029/2003WR002567

Schulz, C. (2007). Temperature and heat flux. In C. Tropea, A. L. Yarin, & J. F. Foss (Eds.), *Springer handbook of experimental fluid mechanics* pp. 487–561). Berlin, Heidelberg: Springer Berlin Heidelberg.

Simpson, S. C., & Meixner, T. (2012). Modeling effects of floods on streambed hydraulic conductivity and groundwater-surface water interactions. *Water Resources Research*, *48*, W02515. https://doi.org/10.1029/2011WR011022

Stonedahl, S. H., Harvey, J. W., Wörman, A., Salehin, M., & Packman, A. I. (2010). A multiscale model for integrating hyporheic exchange from ripples to meanders. *Water Resources Research*, *46*, W12539. https://doi.org/10.1029/2009WR008865

Thomas, S. A., Newbold, J. D., Monaghan, M. T., Minshall, G. W., Georgian, T., & Cushing, C. E. (2001). The influence of particle size on seston deposition in streams. *Limnology and Oceanography*, *46*(6), 1415–1424.

Tonina, D., de Barros, F. P. J., Marzadri, A., & Bellin, A. (2016). Does streambed heterogeneity matter for hyporheic residence time distribution in sand-bedded streams? *Advances in Water Resources*, *96*, 120–126.

Trauth, N., Schmidt, C., Maier, U., Vieweg, M., & Fleckenstein, J. H. (2013). Coupled 3-D stream flow and hyporheic flow model under varying stream and ambient groundwater flow conditions in a pool-riffle system. *Water Resources Research*, *49*, 5834–5850. https://doi.org/10.1002/wrcr.20442

Vanoni, V. A (1974). Factors determining bed forms of alluvial streams. *Journal of the Hydraulics Division*, *100*(HY3), 363–77.

Wörman, A., Packman, A. I., Marklund, L., Harvey, J. W., & Stone, S. H. (2007). Fractal topography and subsurface water flows from fluvial bedforms to the continental shield. *Geophysical Research Letters*, *34*, L07402. https://doi.org/10.1029/2007GL029426

Woessner, W. W. (2000). Stream and fluvial plain ground water interactions: Rescaling hydrogeologic thought. *Groundwater*, *38*(3), 423–429.

Wohl, E. (2015). Legacy effects on sediments in river corridors. *Earth-Science Reviews*, *147*, 30–53.

Xue, P., Schwab, D. J, Sawtell, R. W, Sayers, M. J, Shuchman, R. A, & Fahnenstiel, G. L (2017). A particle-tracking technique for spatial and temporal interpolation of satellite images applied to Lake Superior chlorophyll measurements. *Journal of Great Lakes Research*, *43*(3), 1–13.